J Intell Robot Syst (2007) 48:525–537
DOI 10.1007/s10846-006-9123-8

UNMANNED SYSTEMS PAPER

On Constrained Nonlinear Tracking Control of a Small Fixed-wing UAV

Wei Ren

Received: 17 November 2006 / Accepted: 27 November 2006 /
Published online: 23 January 2007

Abstract The problem of constrained nonlinear tracking control for a small fixed-wing unmanned air vehicles (UAV) is considered. With the UAV equipped with low-level autopilots, the twelve-state model of the UAV is reduced to a six-state model with heading, air speed, and altitude command inputs. Three different approaches based on the state dependent Riccati equation (SDRE), Sontag's formula, and aggressive selection from a satisficing control set are proposed to design the heading and air speed control commands. Those approaches are compared with each other graphically to show their strength and weakness under different scenarios. High-fidelity simulation results on a six-degree-of-freedom twelve-state fixed-wing UAV model are presented to demonstrate the performance of the three approaches.

Key words control Lyapunov function · SDRE · trajectory tracking · unmanned air vehicle

1 Introduction

Unmanned air vehicles (UAVs) have numerous applications in civilian, military, and homeland security sectors. Advanced control technologies for UAVs have received significant attention in recent years. Research on UAVs includes path planning [1, 2], trajectory optimization [3, 4], and cooperative control [5–7], to name a few.

With a fixed-wing UAV equipped with low-level heading-hold, air speed-hold, and altitude-hold autopilots, the resulting UAV/autopilot model is assumed to be first order for heading and air speed hold, and second order for altitude hold [8].

W. Ren (✉)
Department of Electrical and Computer Engineering,
Utah State University, Logan,
UT 84322-4120, USA
e-mail: wren@engineering.usu.edu

Therefore, the planar kinematic equations of motion for the UAV/autopilot model are similar to those of a nonholonomic wheeled mobile robot.

A nonholonomic wheeled mobile robot serves as an interesting topic for stabilization and tracking. An inherent challenge, identified by Brockett's well-known necessary condition for feedback stabilization [9], is that nonholonomic systems cannot be stabilized via smooth time-invariant state feedback. Current approaches to tracking control of a nonholonomic wheeled mobile robot includes linear model [10, 11], sliding-mode [12], backstepping [13–16], and passivity based approaches [17], to name a few.

In contrast to a nonholonomic wheeled mobile robot, the inherent properties of a fixed-wing UAV impose the input constraints of positive minimum air speed, bounded maximum air speed, and saturated heading rate. As a result, most existing approaches for a nonholonomic wheeled mobile robot are not directly applicable to the UAV problem since negative velocities are allowed in these approaches. In this paper, we consider constrained nonlinear trajectory tracking control of a small fixed-wing UAV.

The main purpose of this paper is to propose and compare three different approaches for nonlinear trajectory tracking control of a fixed-wing UAV equipped with low-level air speed-hold, heading-hold, and altitude-hold autopilots. In particular, the first approach is based on the state dependent Riccati equation (SDRE) methodology [18]. The second approach is based on Sontag's formula [19, 20]. The third approach uses a constrained control Lyapunov function (CLF) and aggressively selects a controller from a satisficing control set. These approaches are compared with each other graphically and in simulation to show relative strength and weakness under different situations. It is worthwhile to mention that while the SDRE methodology and Sontag's formula have been well developed in theory for time-invariant nonlinear systems, their applications to a UAV trajectory tracking problem are rare in the current literature.

2 Problem Statement

With the UAV equipped with low-level autopilots, the twelve-state model of the UAV is reduced to a six-state model with heading, air speed, and altitude command inputs. Letting (x, y), ψ, v, and h denote the inertial position, heading angle, air speed, and altitude of the UAV respectively, the kinematic equations of motion are given by

$$\begin{aligned}
\dot{x} &= v\cos(\psi) \\
\dot{y} &= v\sin(\psi) \\
\dot{\psi} &= \frac{1}{\alpha_\psi}(\psi^c - \psi) \\
\dot{v} &= \frac{1}{\alpha_v}(v^c - v), \\
\ddot{h} &= -\frac{1}{\alpha_{\dot{h}}}\dot{h} + \frac{1}{\alpha_h}(h^c - h),
\end{aligned} \tag{1}$$

where ψ^c, v^c, and h^c are the commanded heading angle, air speed, and altitude to the autopilots, and α_* are positive constants [8, 21].

In the remainder of the paper, we assume that the altitude controller follows the design presented in [6], and focus on the design of the heading and air speed controller. Under the assumption that v converges v^c quickly relative to the time-scale of the other dynamics, the air speed-heading dynamics are adequately modeled by

$$\begin{aligned} \dot{x} &= v^c \cos(\psi) \\ \dot{y} &= v^c \sin(\psi) \\ \dot{\psi} &= \frac{1}{\alpha_\psi}(\psi^c - \psi). \end{aligned} \tag{2}$$

Due to the stall conditions, thrust limitations, and roll angle and pitch rate constraints of a fixed-wing aircraft, the following input constraints are imposed on the UAV:

$$\mathcal{U}_1 = \{0 < v_{min} \leq v^c \leq v_{max} - \omega_{max} \leq \omega^c \leq \omega_{max}\}, \tag{3}$$

where $\omega^c = \frac{1}{\alpha_\psi}(\psi^c - \psi)$, v_{min} and v_{max} denote the minimum and maximum air speed of the UAV, and $\omega_{max} > 0$ denotes the heading rate constraint of the UAV.

We assume that the reference trajectory $(x_r, y_r, \psi_r, v_r, \omega_r)$ generated by a trajectory generator [4] satisfies

$$\begin{aligned} \dot{x}_r &= v_r \cos(\psi_r) \\ \dot{y}_r &= v_r \sin(\psi_r) \\ \dot{\psi}_r &= \omega_r \end{aligned} \tag{4}$$

where v_r and ω_r are piecewise continuous and uniformly bounded. In addition, v_r and ω_r satisfy the following constraints:

$$\begin{aligned} \inf_{t\geq 0} v_r(t) &> v_{min} \\ \sup_{t\geq 0} v_r(t) &< v_{max} \\ \sup_{t\geq 0} |\omega_r(t)| &< \omega_{max}. \end{aligned} \tag{5}$$

Transforming the tracking errors expressed in the inertial frame to the UAV frame, the error coordinates become

$$\begin{bmatrix} x_e \\ y_e \\ \psi_e \end{bmatrix} = \begin{bmatrix} \cos(\psi) & \sin(\psi) & 0 \\ -\sin(\psi) & \cos(\psi) & 0 \\ 0 & 0 & 1 \end{bmatrix} \begin{bmatrix} x_r - x \\ y_r - y \\ \psi_r - \psi \end{bmatrix}.$$

Note that the motivation for this transformation is only to simplify the mathematics so that a constrained CLF can be easily derived.

Accordingly, the tracking error model can be represented as

$$\underbrace{\begin{bmatrix}\dot{x}_e\\ \dot{y}_e\\ \dot{\psi}_e\end{bmatrix}}_{\dot{\chi}} = \underbrace{\begin{bmatrix}\omega_r y_e\\ -\omega_r x_e + v_r \sin(\psi_e)\\ 0\end{bmatrix}}_{f_1(t,\chi)} + \underbrace{\begin{bmatrix}-y_e & -1\\ x_e & 0\\ 1 & 0\end{bmatrix}}_{g_1(\chi)} \underbrace{\begin{bmatrix}u_\omega\\ u_v\end{bmatrix}}_{u}, \tag{6}$$

where $\chi = [x_e, y_e, \psi_e]^T$, $u_\omega = \omega_r - \omega^c$, and $u_v = v^c - v_r \cos(\psi_e)$. Note that the air speed and heading commands to the autopilot are

$$v^c = v_r \cos(\psi_e) + u_v$$
$$\psi^c = \psi + \alpha_\psi(\omega_r - u_\omega).$$

The input constraints under the transformation become

$$\mathcal{U}_2 = \{u_\omega, u_v | \underline{\omega} \le u_\omega \le \bar{\omega}, \underline{v} \le u_v \le \bar{v}\}, \tag{7}$$

where $\underline{\omega} \triangleq \omega_r - \omega_{max}$, $\bar{\omega} \triangleq \omega_r + \omega_{max}$, $\underline{v} \triangleq v_{min} - v_r \cos(\psi_e)$, and $\bar{v} \triangleq v_{max} - v_r \cos(\psi_e)$ are time-varying due to the time-varying nature of v^r and ω^r.

It is shown in [22] that

$$V_0(\chi) = \sqrt{\left(\lambda\psi_e + \frac{y_e}{\sqrt{x_e^2 + y_e^2 + 1}}\right)^2 + 1} + k\sqrt{x_e^2 + y_e^2 + 1} - (1 + k) \tag{8}$$

is a constrained CLF for the system (6) with the input constraints (7) such that $\inf_{u\in\mathcal{U}_2} \dot{V}_0(\chi) \le -W(\chi)$, where $W(\chi)$ is a continuous positive-definite function, $k > \frac{1}{2}$, $\lambda > \kappa$, where κ is a positive constant expressed precisely in [22].

3 Nonlinear Trajectory Tracking Control of a UAV

In this section, we propose three different approaches for nonlinear tracking control of a UAV. The first two approaches do not explicitly account for input constraints. In particular, the first approach is based on the SDRE and the second one is based on Sontag's formula. The third approach explicitly accounts for input constraints. In particular, the controllers are aggressively selected from a satisficing control set.

3.1 SDRE Tracking Controller

The SDRE nonlinear regulator is derived to minimize the performance index

$$J = \frac{1}{2}\int_0^\infty [x^T Q(x)x + u^T R(x)u]\mathrm{dt}$$

for the affine nonlinear system

$$\dot{x} = f(x) + g(x)u, \tag{9}$$

where $x \in \mathbb{R}^n$, $u \in \mathbb{R}^m$, $Q(x) > 0$, $R(x) > 0$, $\forall x$, $f(x) \in C^1$, and $f(0) = 0$.

Motivated by the LQR approach for LTI systems, Eq. (9) can be represented as

$$\dot{x} = A(x)x + B(x)u, \tag{10}$$

where $A(x)x = f(x)$ and $B(x) = g(x)$. Note that the decomposition is possible under the conditions that $f(x)$ is continuously differentially and $f(x) = 0$. In the multivariable case, [18] and references therein show that there is an infinite number of ways to factor $f(x)$ into $A(x)x$ and that $A(x)$ can be parameterized as $A(x, \alpha)$, where α is a vector of free design parameters. However, in order to obtain a valid solution of the SDRE, the pair $(A(x, \alpha), B(x))$ has to be pointwise stabilizable.

Under the condition that the pair $(A(x), B(x))$ is pointwise stabilizable, the nonlinear state feedback control law can be constructed as

$$u_{SDRE} = -R^{-1}(x)B^T(x)P(x)x, \tag{11}$$

where $P(x) > 0$ is obtained by solving the state-dependent Riccati equation

$$A^T P + PA - PBR^{-1}B^T P + Q = 0$$

pointwise at each state x. It has been shown that the SDRE regulator is locally asymptotically stable and suboptimal [18].

Equation (6) can be written as $\dot{\chi} = A(t, \chi)\chi + B(\chi)u$, where $\chi = [x_e, y_e, \psi_e]^T$, $u = [u_\omega, u_v]^T$,

$$A(t, \chi) = \begin{bmatrix} 0 & \omega_r(t) & 0 \\ -\omega_r(t) & 0 & v_r(t)\frac{\sin(\psi_e)}{\psi_e} \\ 0 & 0 & 0 \end{bmatrix}$$

and

$$B(\chi) = \begin{bmatrix} -y_e & -1 \\ x_e & 0 \\ 1 & 0 \end{bmatrix}.$$

It can be seen that the pointwise controllability matrix is given by

$$\begin{aligned} C(t, \chi) &= [B(\chi), A(t, \chi)B(\chi), A(t, \chi)^2 B(\chi)] \\ &= \begin{bmatrix} -y_e & -1 & \omega_r x_e & 0 & \omega_r^2 y_e + \omega_r v_r \frac{\sin(\psi_e)}{\psi_e} & \omega_r^2 \\ x_e & 0 & \omega_r y_e + v_r \frac{\sin(\psi_e)}{\psi_e} & \omega_r & -\omega_r^2 x_e & 0 \\ 1 & 0 & 0 & 0 & 0 & 0 \end{bmatrix}. \end{aligned}$$

Note that $v_r(t) > 0, \forall t \geq 0$. It can be verified that $C(t, \chi)$ has full rank when $\omega_r(t) \neq 0$. When $\omega_r(t) = 0$ at some time $t = t^*$, it can be seen that $C(t, \chi)$ still has full rank if and only if $\psi_e \neq k\pi$, $k \in \mathbf{Z} \setminus 0$. As a result, $(A(t, \chi), B(\chi))$ is pointwise controllable as long as $\psi_e \neq k\pi$, $k \in \mathbf{Z} \setminus 0$.

Note that unlike the standard SDRE regulation problem, $A(t, \chi)$ factorized from Eq. (9) is an explicit function of time since the reference air speed $v_r(t)$ and reference heading rate $\omega_r(t)$ are time-varying. The SDRE tracking controller will be obtained by following Eq. (11) except that the pointwise solution to the SDRE, denoted as $P(t, \chi)$, is also an explicit function of time in this case. This results from the fact that the state is regulated to a time-varying trajectory instead of a constant reference state.

Define a saturation function as

$$\text{sat}(\alpha, \beta, \gamma) = \begin{cases} \beta, & \alpha < \beta \\ \alpha, & \beta \leq \alpha \leq \gamma \\ \gamma, & \alpha > \gamma \end{cases},$$

where it is assumed that $\beta < \gamma$. Note that the control $u_{SDRE} = [u_k, u_\ell]^T$ may not satisfy the input constraints (7). The actual control will be saturated to satisfy (7) according to a simple projection as follows:

$$\begin{aligned} u_\omega &= \text{sat}(u_k, \underline{\omega}, \bar{\omega}) \\ u_v &= \text{sat}(u_\ell, \underline{v}, \bar{v}). \end{aligned} \tag{12}$$

3.2 Tracking Controller Based on Sontag's Formula

For the system (9), a globally asymptotically stabilizing control law known as Sontag's formula [19, 20] is given by

$$u_s = \begin{cases} -\frac{L_f V + \sqrt{(L_f V)^2 + (L_g V (L_g V)^T)^2}}{L_g V (L_g V)^T} (L_g V)^T, & L_g V \neq 0 \\ 0, & L_g V = 0 \end{cases} \tag{13}$$

where $V(x)$ is a CLF for the system (9).

The tracking controller based on Sontag's formula can be defined according to Eq. (13) with $L_f V = \frac{\partial V_0}{\partial \chi} f_1(t, \chi)$ and $L_g V = \frac{\partial V_0}{\partial \chi} g_1(\chi)$, where $V_0(\chi)$ is the constrained CLF given by (8). Note that although the universal formula (13) is originally proposed for time-invariant nonlinear systems, the formula is also valid for the time-varying nonlinear system (6) due to the fact that the CLF for the system (6) is not an explicit function of time. However, there is no guarantee that the control $u_s(t, \chi)$ given by Eq. (13) will satisfy the input constraints (7) since Sontag's formula is based on the assumption that $u \in \mathbb{R}^m$. Similar to the SDRE controller, the actual control is a projection of $u_s(t, \chi) = [u_m, u_n]^T$ to the space defined by the input constraints (7) as follows

$$\begin{aligned} u_\omega &= \text{sat}(u_m, \underline{\omega}, \bar{\omega}) \\ u_v &= \text{sat}(u_n, \underline{v}, \bar{v}). \end{aligned} \tag{14}$$

3.3 Tracking Controller Selected from a Satisficing Control Set

Motivated by [23], we define a satisficing control set as

$$\mathcal{F}(t, \chi) = \{u \in \mathcal{U}_2 | L_f V + L_g V u \leq -W(\chi)\},$$

where $L_f V$ and $L_g V$ are defined the same as in Section 3.2, and $W(\chi)$ is the continuous positive-definite function such that $\inf_{u \in \mathcal{U}_2} \dot{V}(\chi) \leq -W(\chi)$. Note that $\mathcal{F}(t, \chi)$ denotes the stabilizing controls at time t (with respect to $V_0(\chi)$) that also satisfy the input constraints (7). Also note that the fact that V is a constrained CLF for the system (6) guarantees that $\mathcal{F}(t, \chi)$ is nonempty for any t and χ.

Define a signum-like function as

$$\operatorname{sgn}(\alpha, \beta, \gamma) = \begin{cases} \beta, & \alpha < 0 \\ \alpha, & \alpha = 0 \\ \gamma, & \alpha > 0 \end{cases}.$$

Let a discontinuous controller $u_d = [u_\omega, u_v]^T$ be defined as

$$\begin{aligned} u_\omega &= \operatorname{sgn}(-\sigma_\omega, \underline{\omega}, \bar{\omega}) \\ u_v &= \operatorname{sgn}(x_e, \underline{v}, \bar{v}), \end{aligned} \tag{15}$$

where $\sigma_\omega \triangleq \lambda\psi_e + \frac{y_e}{\sqrt{x_e^2+y_e^2+1}}$. It can be verified that u_ω and u_v defined above guarantee that $V_0(\chi)$ is a valid Lyapunov function such that $\dot{V}_0(\chi)$ is negative definite.

In [22], a saturation controller $u_{sat} = [u_\omega, u_v]^T$ aggressively selected from the satisficing control set is given by

$$\begin{aligned} u_\omega &= \operatorname{sat}(-\eta_\omega\sigma_\omega, \underline{\omega}, \bar{\omega}) \\ u_v &= \operatorname{sat}(\eta_v x_e, \underline{v}, \bar{v}), \end{aligned} \tag{16}$$

where $\sigma_\omega \triangleq \lambda\psi_e + \frac{y_e}{\sqrt{x_e^2+y_e^2+1}}$, and $\eta_\omega, \eta_v > 0$. It has been shown in [22] that the above control law globally asymptotically stabilizes the system (6) with the input constraints (7) for sufficiently large $\eta_v > 0$ and $\eta_\omega > 0$ expressed precisely in [22].

3.4 Graphical Comparison of the Three Approaches

The different approaches can be compared graphically as shown in Figs. 1 and 2. The line denoted by $L_gVu + L_fV + W = 0$ separates the 2-D control space into

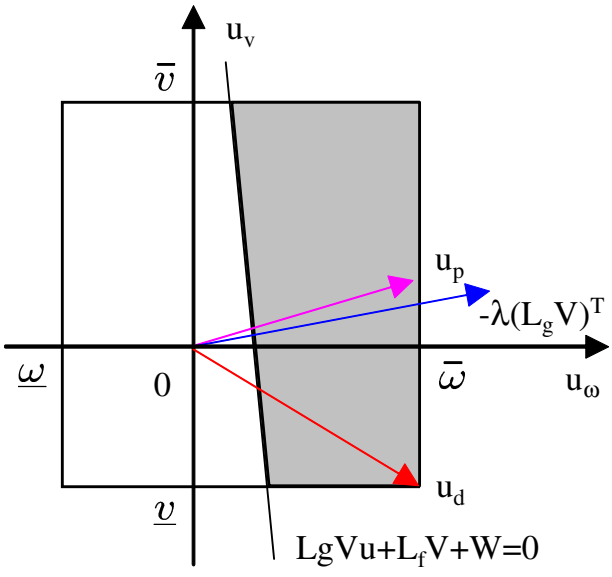

Fig. 1 The satisficing control set $\mathcal{F}(t, \chi)$ at time $t = t_1$

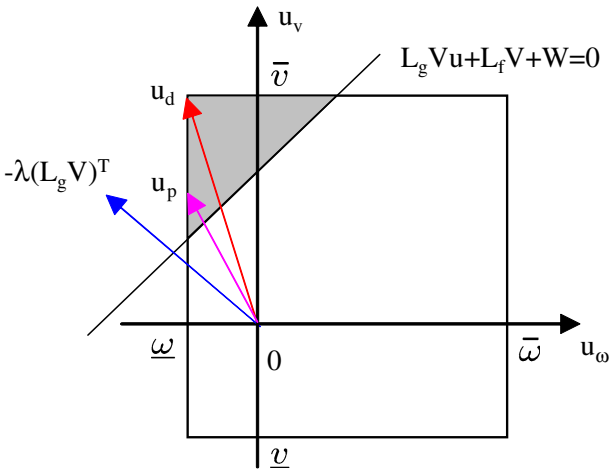

Fig. 2 The satisficing control set $\mathcal{F}(t, \chi)$ at time $t = t_2$

two halves, where the right half in Fig. 1 and the left half in Fig. 2 represent the unconstrained stabilizing controls (with respect to $V_0(\chi)$) satisfying $\dot{V}_0(\chi) \leq -W(\chi)$ at time t_1 and t_2, respectively. The rectangle areas denote the time-varying input constraints (7). The shaded areas in Figs. 1 and 2 represent the satisficing control set $\mathcal{F}(t, \chi)$ at time $t = t_1$ and $t = t_2$, respectively.

In Figs. 1 and 2 the discontinuous controller u_d corresponds to a vertex of a corner of the satisficing control set. The saturation controller u_{sat} corresponds to a point within the satisficing control set. To illustrate, we also plot the vector $-\lambda(L_g V)^T$ in both figures, where $\lambda > 0$. Note that this vector is orthogonal to the line $L_g V u + L_f V + W = 0$. It can be verified that the control based on Sontag's formula can be represented as $u_s(t, \chi) = -\rho(t, \chi)(L_g V)^T$, where $\rho(t, \chi)$ is a nonnegative scalar function of t and χ. Therefore, $u_s(t, \chi)$ lies along the vector $-\lambda(L_g V)^T$ but may have a different magnitude.

In Fig. 1, we can see that the control based on Sontag's formula may or may not stay in the satisficing control set depending on its magnitude. However, a proper scale of the control can always bring it back to the satisficing control set. With the input constraints (7), the actual control will be a projection of $u_s(t, \chi)$ to the rectangle region. As shown in Fig. 1, a projection of $u_s(t, \chi)$, denoted as u_p, is either inside the satisficing control set or on the boundary of the satisficing control set depending

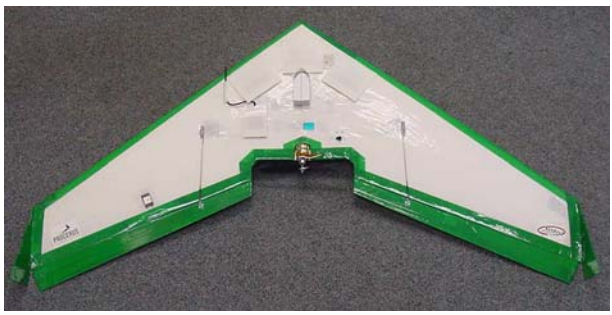

Fig. 3 The 48-inch wingspan UAV at Utah State University

Table 1 Specifications of the UAV and the control law parameters

Parameter	Value
$v_{\min}$	7.5 (m/s)
$v_{\max}$	13.5 (m/s)
$\omega_{\max}$	0.671 (rad/s)
v_r	$\in$ [9.5, 11.5] (m/s)
ω_r	$\in$ [−0.471, 0.471] (rad/s)
λ	1
η_v	1
η_ω	1

on its magnitude. In either case, the projected control based on Sontag's formula guarantees stability even if there are input constraints. In Fig. 2, we can see that the control based on Sontag's formula cannot stay within the satisficing control set even with some scaling due to its direction. In this case, a projection of $u_s(t, \chi)$ is not guaranteed to stay within the satisficing control set. However, it is straightforward to see that $\nu u_s(t, \chi)$, where $\nu > 1$, is still a stabilizing control in the case of $u \in \mathbb{R}^m$. As a result, for a stabilizing control $\nu u_s(t, \chi)$ with significantly large magnitude, the projection of $\nu u_s(t, \chi)$ to the rectangle area, denoted as u_p, is guaranteed to be on the

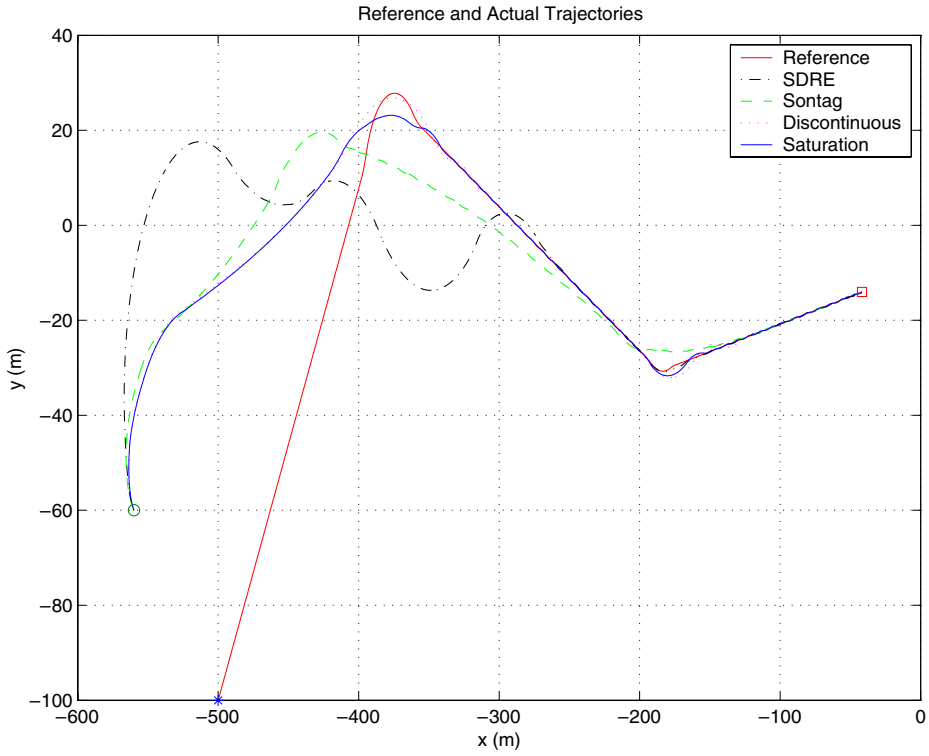

Fig. 4 The reference and actual trajectories using the air speed and heading controllers

boundary of the satisficing control set as shown in Fig. 2, which in turn guarantees stability.

The projection of the SDRE control u_{SDRE} to the rectangle area is not guaranteed to be within the satisficing control set since the SDRE control may not be stable with respect to the Lyapunov function $V_0(\chi)$. In fact, the SDRE control may not guarantee global stability even with unconstrained control inputs. That is, the SDRE control may not even point toward the unconstrained stabilizing area. Of course, this disadvantage can be corrected by projecting the SDRE control to the satisficing control set rather than the entire constrained input space at each time. In this paper, we still project the SDRE control to the entire constrained input space as given by Eq. (12) for comparison purposes.

4 Simulation Results

In this section, we simulate a Zagi airframe (http://zagi.com) based UAV that tracks a time-parameterized reference trajectory generated by the trajectory generator described in [4], where the reference trajectory satisfies the constraints (5). The simulation results in this section are based on a full six degree-of-freedom twelve-state high-fidelity UAV model equipped with low-level autopilots described in [21].

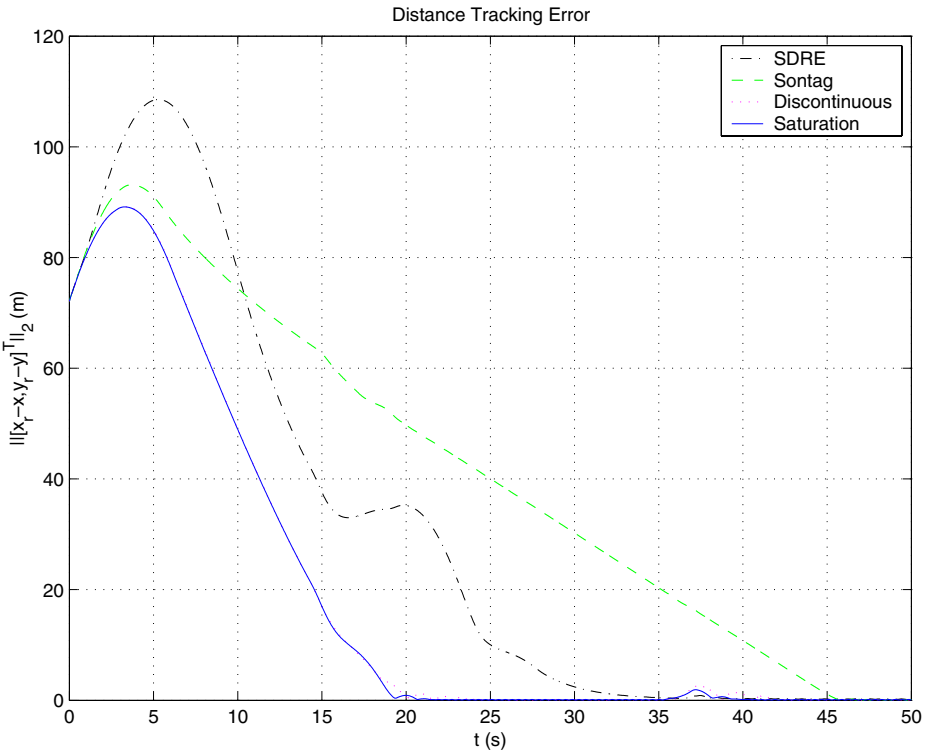

Fig. 5 The distance tracking errors using the air speed and heading controllers

All of the simulation parameters are derived from a 48-inch wingspan Procerus UAV platform shown in Fig. 3.

We apply the air speed and heading commands derived in Section 3 to the 6-DOF 12-state UAV model. Table 1 shows the specifications of the UAV and the control law parameters.

Figure 4 shows the reference trajectory generated by the trajectory generator and the actual trajectories generated by the four tracking controllers described in Section 3. Here we use circles and squares to represent the starting and ending position of the UAV, respectively. In addition, a star and a square are used to represent the starting and ending position of the reference trajectory, respectively. For the SDRE controller, the weighting matrices are chosen as $Q(x) = \text{diag}([1, 1, 1])$ and $R(x) = \text{diag}([8, 10])$. In terms of tracking speed, the saturation and discontinuous controllers produce the fastest tracking while the controller based on Sontag's formula produces the slowest tracking.

Figures 5 and 6 show the distance and heading tracking errors of the UAV, respectively. We can see that all four controllers guarantee asymptotic tracking. However, it can be seen that the saturation controller and the discontinuous controller are superior to the SDRE controller and the controller based on Sontag's formula. This is due to the fact that the saturation controller and the discontinuous controller explicitly account for the input constraints during their design procedures. In fact, the

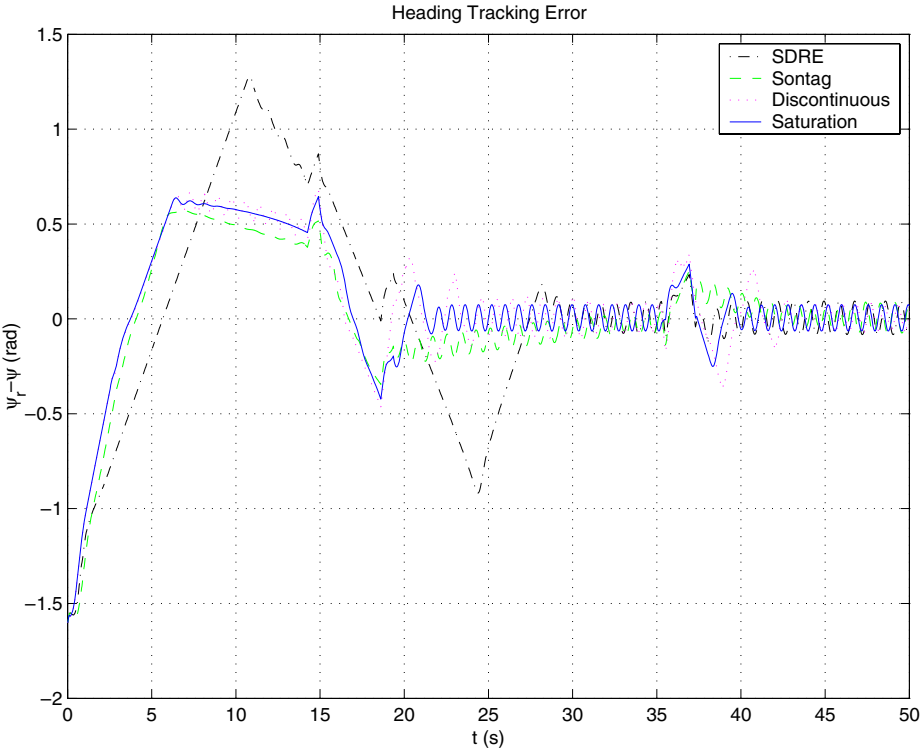

Fig. 6 The heading tracking errors using the air speed and heading controllers

SDRE controller has the worst performance for heading tracking due to the heading rate saturation.

During the test, we have also noticed that the SDRE controller can achieve better performance than the saturation controller under small initial tracking errors by properly choosing the weighting matrices $Q(x)$ and $R(x)$, which is due to the fact that the SDRE controller is proved to be locally asymptotically stable and suboptimal. However, generally the performance of the SDRE controller is degraded dramatically under large initial tracking errors due to the input constraints.

5 Conclusion and Future Work

Trajectory tracking control for a small fixed-wing UAV equipped with low-level autopilots has been studied. Non-CLF based control approach and CLF based control approaches are applied to derive heading and air speed commands to achieve asymptotical tracking. High-fidelity simulation results on a 6-DOF 12-state small fixed-wing UAV model have shown the performance of different controllers for trajectory tracking. Future work includes implementing the controllers on a 48-inch wingspan fixed-wing UAV.

Acknowledgements The author would like to gratefully acknowledge Prof. Randy Beard, Prof. Tim McLain, and Mr. Derek Kingston for their technical guidance on the subject.

References

1. Faiz, N., Agrawal, S.K., Murray, R.M.: Trajectory planning of differentially flat systems with dynamics and inequalities. AIAA J. Guid. Control Dyn. **24**(2), 219–227 (2001)
2. Frazzoli, E., Dahleh, M.A., Feron, E.: Real-time motion planning for agile autonomous vehicles. AIAA J. Guid. Control Dyn. **25**(1), 116–129 (2002)
3. Yakimenko, O.A.: Direct method for rapid prototyping of near-optimal aircraft trajectories. AIAA J. Guid. Control Dyn. **23**(5), 865–875 (2000)
4. Anderson, E.P., Beard, R.W., McLain, T.W.: Real time dynamic trajectory smoothing for uninhabited aerial vehicles. IEEE Trans. Control Syst. Technol. **13**(3), 471–477 (2005)
5. Giulietti, F., Pollini, L., Innocenti, M.: Autonomous formation flight. IEEE Control Syst. Mag. **20**(6), 34–44 (2000)
6. Beard, R.W., McLain, T.W., Goodrich, M., Anderson, E.P.: Coordinated target assignment and intercept for unmanned air vehicles. IEEE Trans. Robot. Autom. **18**(6), 911–922 (2002)
7. McLain, T.W., Beard, R.W.: Coordination variables, coordination functions, and cooperative timing missions. AIAA J. Guid. Control Dyn. **28**(1), 150–161 (2005)
8. Proud, A.W., Pachter, M., D'Azzo, J.J.: Close formation flight control. In: Proceedings of the AIAA Guidance, Navigation, and Control Conference, Portland, OR, pp 1231–1246, Paper No.AIAA-99-4207 (1999)
9. Brockett, R.W.: Asymptotic stability and feedback stabilization. In: Millman, R.S., Sussmann, H.J. (eds.) Differential Geometric Control Theory, pp. 181–191. Birkhaüser, Cambridege, MA (1983)
10. Bloch, A.M., McClamroch, N.H., Reyhanoglu, M.: Controllability and stabilizability properties of a nonholonomic control system. In: Proceedings of the 29th Conference on Decision and Control, Honolulu, HI, pp. 1312–1314 (1990)
11. Divelbiss, A.W., Wen, J.T.: Trajectory tracking control of a car-trailer system. IEEE Trans. Control Syst. Technol. **5**(3), 269–278 (1997)
12. Yang, J.M., Kim, J.H.: Sliding mode motion control of nonholonomic mobile robots. Control Syst. Mag. **19**(2), 15–23 (1999)

13. Fierro, R., Lewis, F.L.: Control of a nonholonomic mobile robot: backstepping kinematics into dynamics. In: Proceedings of the 34th Conference on Decision and Control, New Orleans, LA, pp. 3805–3810 (1995)
14. Jiang, Z.P., Nijmeijer, H.: Tracking control of mobile robots: a case study in backstepping. Automatica **33**, 1393–1399 (1997)
15. Fukao, T., Nakagawa, H., Adachi, N.: Adaptive tracking control of a nonholonomic mobile robot. IEEE Trans. Robot. Autom. **16**(5), 609–615 (2000)
16. Lee, T.C., Song, K.T., Lee, C.H., Teng, C.C.: Tracking control of unicycle-modeled mobile robots using a saturation feedback controller. IEEE Trans. Control Syst. Technol. **9**(2), 305–318 (2001)
17. Jiang, Z.P., Lefeber, E., Nijmeijer, H.: Saturated stabilization and track control of a nonholonomic mobile robot. Syst. Control Lett. **42**, 327–332 (2001)
18. Cloutier, J.R.: State-dependent Riccati equation techniques: an overview. In: Proceedings of the American Control Conference, pp. 932–936 (1997)
19. Sontag, E.D.: A 'universal' construction of Artstein's theorem on nonlinear stabilization. Syst. Control Lett. **13**, 117–123 (1989)
20. Krstić, M., Deng, H.: Stabilization of Nonlinear Uncertain Systems. Communication and Control Engineering. Springer, Berlin Heidelberg New York (1998)
21. Kingston, D., Beard, R., McLain, T., Larsen, M., Ren, W.: Autonomous vehicle technologies for small fixed wing UAVs. In: AIAA 2nd Unmanned Unlimited Systems, Technologies, and Operations–Aerospace, Land, and Sea Conference and Workshop & Exhibit, San Diego, CA, paper no. AIAA-2003-6559 (2003)
22. Ren, W., Beard, R.W.: Trajectory tracking for unmanned air vehicles with velocity and heading rate constraints. IEEE Trans. Control Syst. Technol. **12**(5), 706–716 (2004)
23. Curtis, J.W., Beard, R.W.: Satisficing: A new approach to constructive nonlinear control. IEEE Trans. Autom. Control **49**(7), 1090–1102 (2004)